NÖHÜ Müh. Bilim. Derg. / NOHU J. Eng. Sci., 2021; 10(1): 063- 070

Niğde Ömer Halisdemir Üniversitesi Mühendislik Bilimleri Dergisi
Niğde Ömer Halisdemir University Journal of Engineering Sciences
ISSN: 2564-6605
Araştırma / Research

# A modular buck-boost drive system for torque ripple minimization of switched reluctance machines

## Anahtarlamalı relüktans makinalarının moment salınımı minimizasyonu için modüler bir yükseltici-alçaltıcı sürücü sistemi

**Burak Tekgün** [1,*]

[1] *Abdullah Gül University, Department of Electrical-Electronics Engineering, 38080, Kayseri, Turkey*

**Abstract**

*In this paper, a modular three-phase buck-boost switched reluctance machine (SRM) drive system is proposed. In this topology, the three-phase SRM drive is composed of three single-phase modules that are connected in parallel where each single-phase inverter module is formed with a bidirectional buck-boost DC/DC converter and a cascaded H-bridge inverter. The DC/DC converter generates the rectified form of the phase voltage and the H-bridge inverter alternates and controls the polarity of the output voltage. This structure allows one to adjust the phase voltages independently, which provides faster excitation and demagnetization for a wide range of operating conditions. Since the voltage is always regulated dynamically, the need for bulky DC-bus capacitors is eliminated; hence, the size and the cost of the drive system are reduced. To validate the superiority of the proposed system and compare it with the traditional one, a set of simulations are done in MATLAB®/Simulink®. Not only the torque ripple is reduced, but also a higher torque per ampere ratio is achieved with the proposed system.*

**Keywords:** Fast excitation and demagnetization, Modular motor drive, Switched reluctance motor (SRM)

**Özet**

*Bu makalede modüler yapıda olan üç fazlı bir alçaltıcı yükseltici anahtarlamalı relüktans motoru sürücü (ARM) sistemi önerilmiştir. Bu topolojide üç fazlı ARM sürücü üç adet tek-fazlı modülün paralel bağlanmasıyla oluşturulmuş olup, her tek-fazlı sürücü bir çift yönlü çalışan alçaltıcı-yükseltici DA/DA dönüştürücü ve bunun sonrasına bağlanmış bir H-köprü eviriciden oluşmaktadır. DC/DC dönüştürücü faz geriliminin doğrultulmuş formunu oluşturmakta ve H-köprülü evirici de oluşturulan gerilimin yönünü değiştirerek çıkış geriliminin polaritesini kontrol etmektedir. Bu yapı faz gerilimlerinin birbirinden bağımsız olarak ayarlanmasına önayak olarak, hızlı enerjilenmeyi ve demagnetizasyonu mümkün kılmaktadır. Bunun sonucunda komütasyon performansı iyileştirilmiş ve moment salınımı azaltılmıştır. Gerilim dinamik olarak sürekli regüle edildiğinden büyük DC-bara kondansatörlerine olan ihtiyaç ortadan kalkmış ve böylece sürücü boyutu ve maliyeti azaltılmıştır. Önerilen sistemin üstünlüğünü doğrulamak ve bu sitemi geleneksel sistemle karşılaştırmak üzere MATLAB®/Simulink® ortamında bir dizi benzetim çalışması yapılmıştır. Önerilen sistem ile sadece moment salınımı azaltılmamış daha yüksek bir amper başına moment oranı da elde edilmiştir.*

**Anahtar Kelimeler:** Hızlı enerjilenme ve demagnetizasyon, Modüler motor sürücü, Anahtarlamalı relüktans motoru (ARM)

## 1 Introduction

Switched reluctance machines (SRM) are drawing increasing attention worldwide due to the features that come from their simplicity. SRMs have the simplest geometry to be manufactured, they are cheap, reliable, robust, being suitable to be used in harsh environments, and free of rare earth magnets [1, 2]. In terms of power density and efficiency, they are comparable to the induction machines (IM). On the other hand, their doubly salient structure and highly nonlinear magnetization characteristics make a high torque output ripple inevitable. Due to the high torque ripple and the excitation current`s high-frequency harmonic components, SRMs are having acoustic noise and vibration issues [3, 4]. Therefore, parameters that affect the performance measures such as turn-on/off angles (commutation), current regulation, DC bus voltage adjustments should be treated properly [5, 6]. During the last decades, numerous research has been reported on converter topologies and control methods for improving the performance and operating range, as well as the torque ripple and acoustic noise reduction [2, 7, 8].

Among many SRM converter structures, asymmetric-bridge converter topology is considered as the traditional SRM drive. In this topology, each phase current is controlled with two active switches and two diodes using the hysteresis current regulation technique. Although it provides a flexible operation and high-performance current regulation, the switching frequency is not controlled which results in high switching losses and oversized inverter designs [1]. In order to achieve high performance at a wide range of operating conditions, various DC bus voltage boosting or regulating SRM drive topologies are developed for the grid and battery-powered systems [6, 9–13] which possess the advantages of reduced DC bus capacitor size, reduced voltage variation effects on the control system, improved commutation capability, extended driving range, increased output power [9].

One of the most used topologies is the C-dump converter that improves the turn-on and turn-off characteristics [11], [14, 15]. The C-dump converter charges a capacitor that is connected series to the DC bus during the demagnetization. Later, the additional capacitor voltage is used to excite and/or demagnetize the next phase of the SRM. In [16], a battery-powered electric vehicle (EV) SRM drive system is

* Sorumlu yazar / Corresponding author, e-posta / e-mail: burak.tekgun@agu.edu.tr (B. Tekgün)
Geliş / Recieved: 06.10.2020… Kabul / Accepted: 13.12.2020 Yayımlanma / Published: 15.01.2021
doi: 10.28948/ngmuh.806323

developed with the C-dump converter. In [17], the effect of the voltage boost during the demagnetization is analyzed, and improved performance in terms of average torque and power output is reported. The hybrid excitation where two phases are kept turned on with the help of a C-dump converter is proposed in [12]. The biggest disadvantage of C-dump converters is the additional capacitor voltage level is highly dependent on the operating condition, for instance, if the machine is generating a high torque the voltage boost will be high, and vice versa. Consequently, high power and high-speed operations are limited. Additionally, the reliability of this converter is poor as it does not have a fault-tolerant ability due to its non-isolated structure [10]. It is possible to find other types of approaches in the literature. In [10], a multilevel converter topology is proposed for plug-in hybrid EVs, where the battery bank is used to elevate the DC bus voltage for faster excitation and demagnetization. A voltage boosting converter topology is reported in [9], which is also able to operate during the charging from the grid with power factor correction (PFC) feature. A bidirectional buck-boost topology is used for EV driving and charging operations in [18]. In [19], a four-phase modified Miller converter as an SRM drive is proposed where the elevated DC bus voltage provides a wide range of shifted commutation angle, consequently, high-speed performance is improved. In [11], an SRM drive system that operates in a vehicle-home-grid network, which is formed with a front end bidirectional two-quadrant DC/DC converter and an asymmetric drive is reported. In addition to the above studies, there exist some studies that take battery management issues into consideration, which improved the stability, fault-tolerant ability, and eventually, the reliability [20–22].

Using any aforementioned drive systems does not guarantee maximized efficiency. To maximize the SRM efficiency, the average output torque should be maximized for each given RMS amps, namely torque per ampere ratio, $T_{avg}/I_{RMS}$, should be maximized [5]. Numerous control schemes are proposed to address this issue such as optimal turn-on, turn-off angle determination [5], hybrid excitation [12], and various torque sharing methods [23], [24]. The success of these methods mostly depends on the successful current regulation. Due to the nonlinear magnetic characteristics of the SRM, it is a challenge to conduct an accurate current regulation. Simple average PI control [14], hysteresis control, DQ control [7], [25], sliding mode control [26], back emf predictive control [27] are some of these structures.

In this paper, a modular buck-boost SRM drive system is proposed, where each phase has its non-inverting buck-boost converter and an H-bridge converter. The system works in torque control mode and reference phase currents are regulated with PI controllers in the hybrid manner where two-phase operated at the same time during the commutation. The output of the PI regulator is the reference voltage to be generated by the DC/DC buck-boost converter, then, the polarity of the generated voltage is controlled with the cascaded H-bridge inverter. The proposed topology is able to step up or down the DC input voltage; hence, a faster excitation and demagnetization is possible, which leads to a reduced torque ripple, increased output torque and power, and extended speed range. Also, this structure helps to eliminate the large DC bus capacitors, reduces the switching losses as the high frequency switching only occurs at the DC/DC conversion stage, and lengthens the machine lifetime by deducting the current-stress in the machine windings. Moreover, the proposed system is a modular structure that provides great flexibility. Different SRM configurations like three, four, or more-phase SRMs can be driven by just adding a module for each phase; higher power levels can be achieved by adding parallel converters.

This paper is organized as follows: The proposed modular buck-boost SRM drive system is presented and analyzed in Section II, where the SRM drive operating modes, module topology, the control system, and the complete SRM drive system are given in detail. In Section III, the simulation study is explained in detail, the results are provided, and the conclusions are made in Section V.

## 2 Proposed Modular Buck-Boost SRM Drive System

The single-phase control of a conventional asymmetric SRM drive is presented in Figure 1, where $V_{DC}$ is the DC input voltage, $C_{DC}$ is the DC/DC converter input capacitor, $S_L$ and $S_H$ are the upper and lower switches, $L_{phase}$, $r_L$, and $emf$ are the phase inductance, phase resistance and the back emf component of the SRM. The same structure is repeated for each phase. The asymmetric converter has an inherent shoot through fault feature by having an active switch and a diode on each leg [28]. This simple structure allows the circuit operates in three modes namely, excitation, free-wheeling, and demagnetization modes as illustrated in Figure 2. In the excitation mode, both lower and upper switches are turned on to apply the supply voltage; in the free-wheeling mode, either the lower or upper switch is turned to apply zero voltage; and in demagnetization mode, both switches are turned off to force diodes to conduct and apply negative supply voltage to the SRM windings.

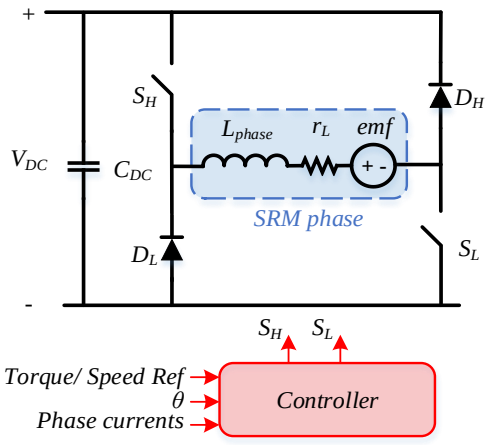


**Figure 1.** Single-phase control of a conventional asymmetric SRM drive.

In this topology, the current control through hysteresis current regulation or any other PWM technique can be

achieved easily where the machine speed is relatively low. However, it gets harder to regulate the phase currents accurately as the speed and the back emf voltage increase. As mentioned before, various voltage boosting topologies and shifting techniques are proposed to overcome this issue.

The proposed topology is made of a modular structure where all the phases are controlled with separate modules that can step up and down the voltage whenever it is necessary. The following subsections provide details of the module topology, the module control system, and the whole modular SRM drive system.

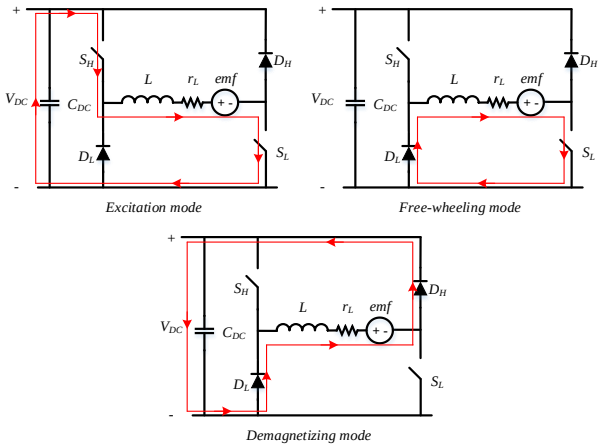


**Figure 2.** Operating modes of conventional asymmetric SRM drive.

### *2.1 Module topology*

The single-phase modules are made out of a bidirectional non-inverting buck-boost converter that has four switches with body diodes and an H-bridge inverter to alternate the generated voltage as shown in Figure 3, where $L$ and $C$ are the DC/DC converter inductor and the output capacitor, $D_1$, $D_2$, $D_3$, and $D_4$ are the antiparallel diodes and $S_1$, $S_2$, $S_3$ and $S_4$ are the switching elements of the DC/DC converter, $V_{rAC}$ is the voltage across the output capacitor, also named as rectified AC voltage, $D_5$, $D_6$, $D_7$, and $D_8$ are the antiparallel diodes and $S_5$, $S_6$, $S_7$ and $S_8$ are the switching elements of the H-bridge converter, and $V_{out}$ is the output voltage of the module.

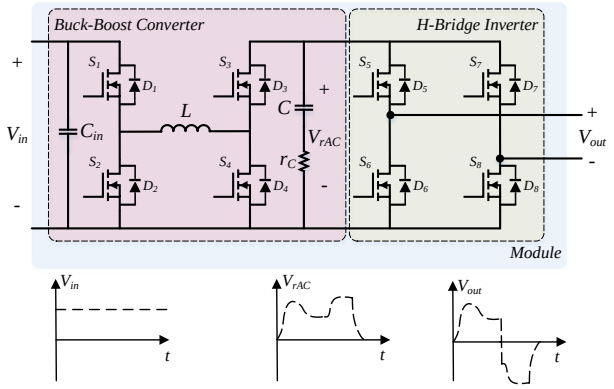


**Figure 3.** The module structure of the proposed SRM drive.

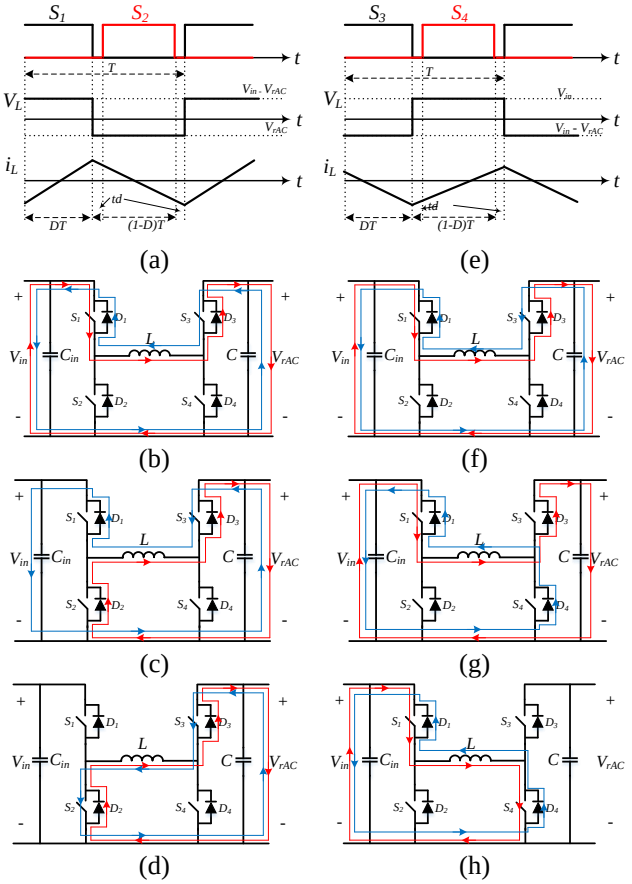

**Figure 4.** In motoring mode (red lines) (a) buck operation switching pattern and the circuit modes when (b) $0 < t < DT$, (c) $DT < t < DT+td$, *and* (d) $DT+td < t < T$; (e) boost operation switching pattern, circuit modes when (f) $0 < t < DT$, (g) $DT < t < DT+td$, *and* (h) $DT+td < t < T$.

The bidirectional buck-boost converter operates in four modes namely, motoring buck/boost, and generating buck/boost modes. In case the converter is operating in motoring mode (shown with red lines in Figure 4) and the buck-boost converter operates in buck mode, the $S_3$ switch is fully turned on and $S_4$ is fully turned off; $S_1$ and $S_2$ switches alternate and form a synchronous buck converter. The switching pattern, inductor voltage and current are given in Figure 4.a. During this operation the circuit modes at the time intervals of $0 < t < DT$, $DT < t < DT+t_d$, *and* $DT+t_d < t < T$ are presented in Figure 4.b, Figure 4.c, and Figure 4.d, respectively. Here, $D$ is the duty ratio, $T$ is the switching period, and $t_d$ is the dead-time. Similarly, for the case where the converter operates as a boost converter when motoring, the $S_1$ switch is fully turned on, $S_2$ is fully turned off, and the $S_3$ and $S_4$ switches alternate to form a synchronous boost converter. The switching pattern, inductor voltage, and current are given in Figure 4.e. During this operation the circuit modes at the time intervals of $0 < t < DT$, $DT < t < DT+t_d$, *and* $DT+t_d < t < T$ are shown in Figure 4.f, Figure 4.g, and Figure 4.h, respectively. The synchronous structure is selected intentionally to minimize the converter losses by eliminating the high power loss from the diodes` conduction loss. Due to the symmetrical structure of the non-inverting

buck-boost converter, the modes of operation during the generation mode will be quite similar as shown with blue lines in Figure 4 except the inductor current direction is different. Therefore, a further explanation for the generating case will not be presented in this paper.

### 2.2 Control system

The proposed buck-boost inverter has an open-loop structure. Switches $S_5$, $S_6$, $S_7$, and $S_8$ are triggered according to the voltage reference polarity, $S_5$ and $S_8$ are turned on if the reference voltage is positive, and $S_6$ and $S_7$ are turned on if it is negative.

After normalizing the reference waveform based on the input voltage, the reference is clamped between 0 and 3 for limiting the drive output voltage for stable and safe operation. $S_1$ and $S_2$ are controlled with further clamping of this signal between 0 and 1 while $S_3$ and $S_4$ are controlled with linearized boost converter duty ratio using a one-dimensional lookup table (LUT). The control system block diagram is presented in Figure 5, the duty ratios versus the normalized reference voltage when it varies between zero and three are shown in Figure 6. This simple control structure allows the power to flow in either direction as this feature is required to drive an SRM considering the power is flowing from the machine to the source and vice versa during the excitation and demagnetization.

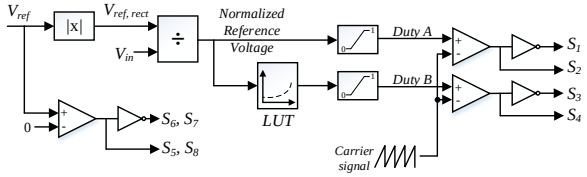


**Figure 5.** The open-loop control structure of the proposed buck-boost inverter.

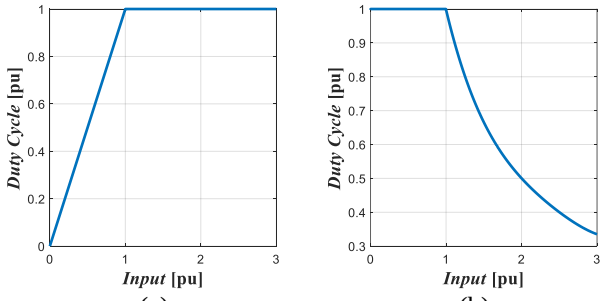


**Figure 6.** (a) Duty cycle of the $S_1$ ($S_2$ alternates) switch vs. the normalized input voltage reference; (b) duty cycle of the $S_3$ ($S_4$ alternates) switch vs. the normalized input voltage reference.

### 2.3 SRM drive system

The proposed three-phase SRM drive system consists of three individual single-phase modules for each SRM phase as shown in Figure 7. This modular structure provides great flexibility, it is possible to drive SRMs having a lower or higher number of phases and having a higher power rating by simply adding more modules to the drive system

The SRM drive system is operated with the torque control structure. This structure can easily be extended to the speed and position control structures by cascading additional controllers. The control structure is given in Figure 8, where the reference torque and optimized turn on and turn off angles along with the rotor position are fed back to the current reference generation block. This block generates the reference currents with a simple structure, where the required current waveform is simply a square waveform whose amplitude is taken from pre-generated torque vs current and position lookup table. Later, these current references go into a PI current regulator that generates the voltage reference. Calculated voltage references fed to the modules and generated voltages by modules are applied to the SRM windings. Modules are acting as a controlled voltage source during the operation.

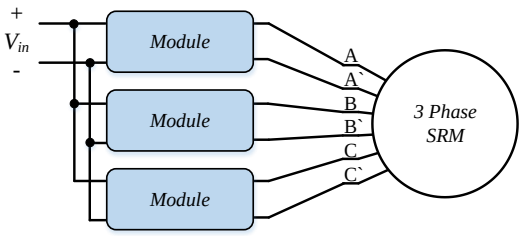


**Figure 7.** The proposed modular three-phase SRM drive system.

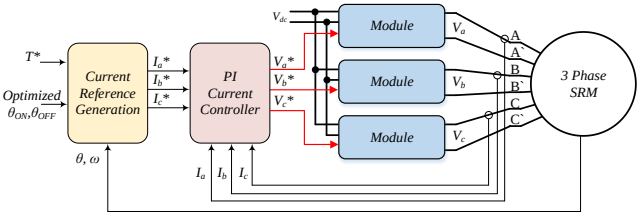


**Figure 8.** SRM torque control block diagram with the proposed drive system.

## 3 Simulations and Results

The SRM used in this work is modeled with two LUTs which are flux linkage vs current vs position and torque vs current vs position. These LUTs are generated using a finite element analysis software, ANSYS/Maxwell. Motor control and modular drive simulation studies are performed in MATLAB®/Simulink®.

The parameters of the SRM used in this study are given in Table 1.

**Table 1**. The Parameters of the SRM used in simulations.

| Parameter | Value |
|---|---|
| Power | 2 kW |
| Base speed | 1000 rpm |
| Rated peak current | 21 A |
| Rated voltage | 200 Vdc |
| Stator/Rotor pole configuration | 24/16 |
| Phase resistance | 0.24 Ω |

The flux linkage vs position vs current, and torque vs position vs current plots are presented in Figure 9a and Figure 9b, respectively.

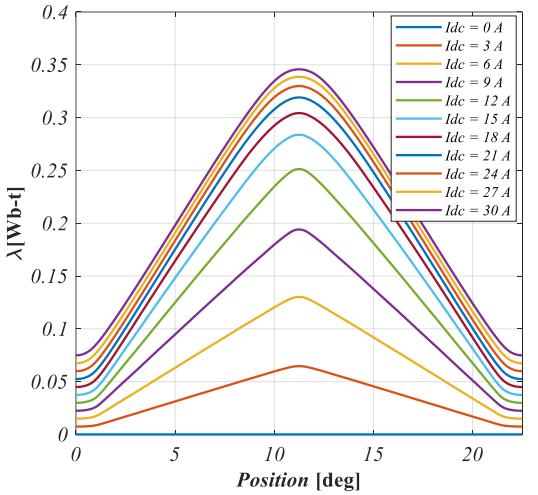


(a)

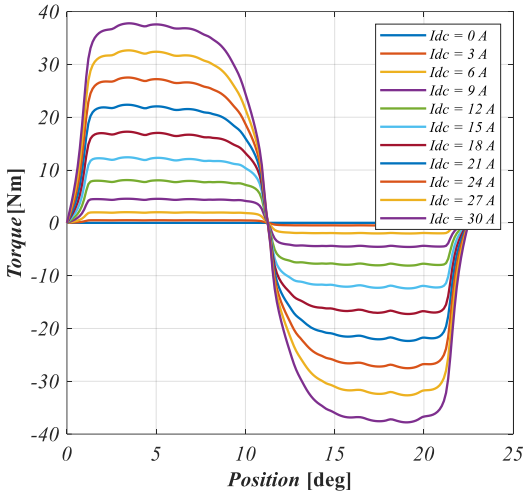


(b)

**Figure 9.** (a) Flux linkage vs position vs current, and (b) torque vs position vs current plots.

The SRM model built in MATLAB®/Simulink® executes the basic terminal equation as following:

$$V = RI + \frac{d\lambda}{dt} \quad (1)$$

where, V is the terminal voltage, R is the phase resistance, I is the phase current, and λ is the flux linkage. The phase current is calculated using (1) and the torque is calculated using the torque vs position vs current LUT. This process is done for each phase to calculate the total torque.

The buck-boost converter of the modules is operated at 100 kHz switching frequency and it has a 100 µH inductor and 10 µF output capacitor. The modules are able to step up the voltage to 600 V dynamically; however, the voltage is limited to 400 for safe operation.

Two simulations were performed to compare the conventional and the proposed SRM drive systems. At 1000 rpm speed the full torque of 20 Nm is tried to be generated. It should be kept in mind that 1000 rpm is the base speed, i.e. at this speed and full torque, the machine is operating at the voltage limit, 200 V input voltage will not be enough for the drive to be able to regulate the phase currents if the machine speeds up or output torque increases.

Firstly, the conventional drive system with hysteresis current control is simulated. The optimized turn-on and turn-off angles are determined as 6.6 and 14.6 degrees by manually sweeping these angles with a series of simulations and the phase currents are generated as shown in Figure 10a. The average steady-state torque is determined as 20 Nm while the peak-to-peak torque variation is 9.37 Nm, which is 46.8% of the average steady-state torque as shown in Figure 10b.

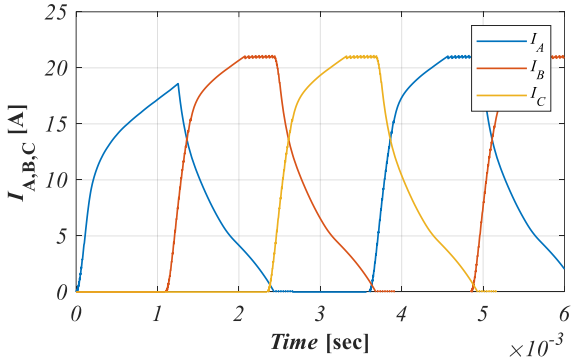


(a)

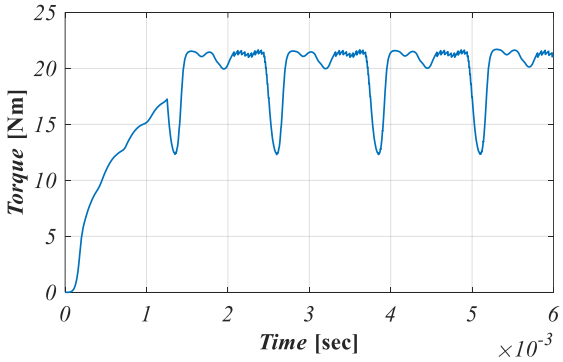


(b)

**Figure 10.** (a) Phase currents and (b) output torque waveforms of the conventional SRM drive system.

The second simulation is done with the proposed SRM drive system. Similar to the conventional system simulation, the input voltage is kept as 200 V but in this case, the voltage can be boosted up to 400 V. The turn on and turn of angles are again determined through a set of simulations as 7.35 and 15.45 degrees. The proposed system generated the phase currents in the hybrid form, where the two phases are kept on for a brief time, hence the torque production is maintained during the commutation. The phase currents are presented in Figure 11a. It is observed that the average steady-state torque

is 21.5 Nm, peak-to-peak torque variation is 1.36 Nm that is 6.3 % of the average torque as shown in Figure 11b.

To regulate the currents in the desired waveforms the current regulators adjusted the phase voltages as given in Figure 12. The hybrid excitation is more obvious in the voltage waveforms. This scheme provides a more balanced excitation and helps reduce the abrupt excitation variations resulting in a lower torque ripple, lower acoustic noise, and vibration.

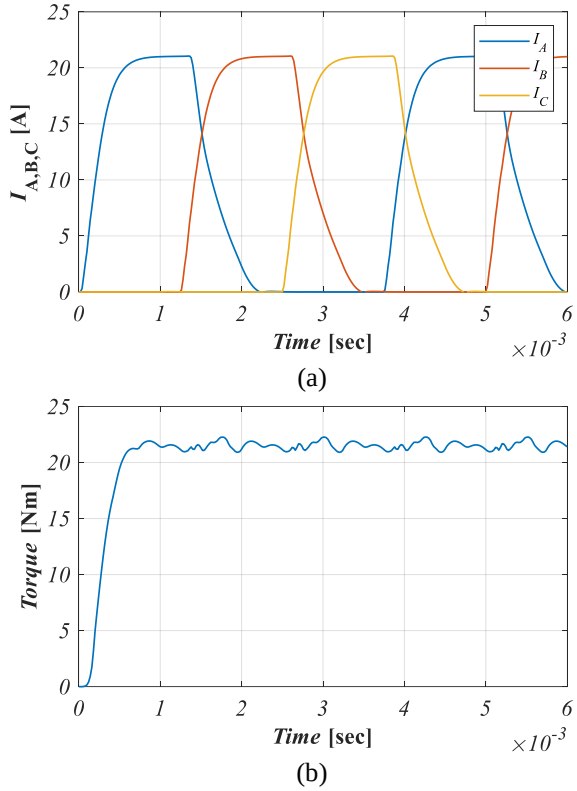


**Figure 11.** (a) Phase currents and (b) output torque waveforms of the proposed SRM drive system.

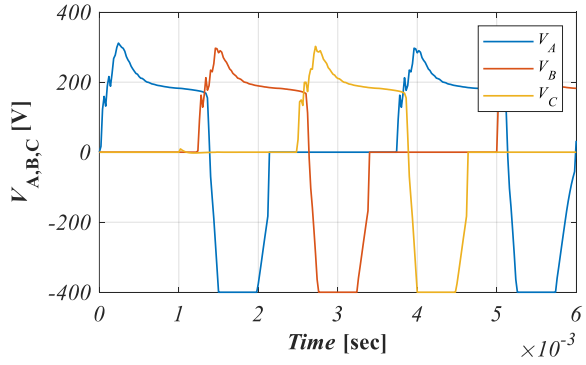


**Figure 12.** Phase voltages of the proposed SRM drive system.

This simulation study is extended to a wider operation range and performance improvements are recorded and presented in Figure 13. The capability curve, percent torque ripple, maximum torque per ampere, and maximum power output for both conventional and proposed drive systems are plotted and compared in Figure 13a, 13b , 13c and 13d, respectively.

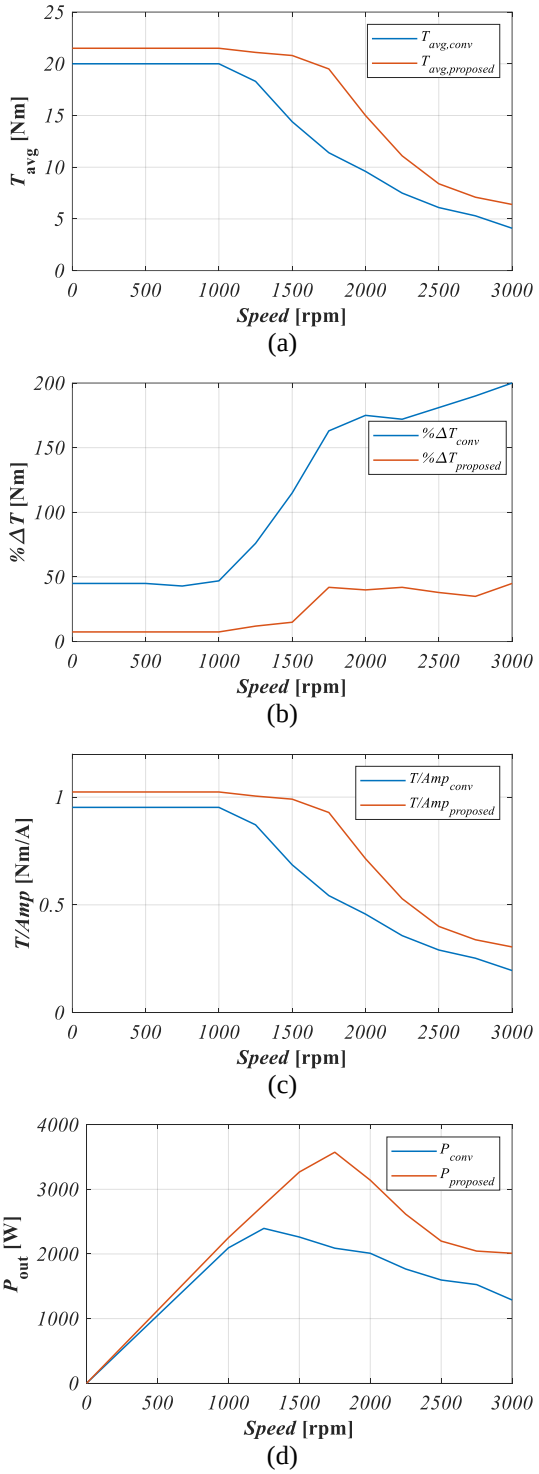


**Figure 13.** (a) The capability curve, (b) percent torque ripple, (c) maximum torque per ampere, and (d) maximum power output curves of conventional and proposed SRM drive systems.

It can be clearly seen from the results that the proposed system greatly reduces the torque ripple, extends the speed range, and improves the torque per ampere performance and

the power output. This work can be extended to a proper torque sharing function development study for even achieving a very low torque ripple at a wide operating range, which would make SRMs a viable and cost-effective option for a variety of applications including domestic and automotive applications.

## 4 Conclusions

In this paper, a modular three-phase buck-boost switched reluctance machine (SRM) drive system is proposed, where a three-phase SRM drive that is composed of three single-phase modules connected in parallel. The single-phase inverter modules are formed with a bidirectional buck-boost DC/DC converter and a cascaded H-bridge inverter. The DC/DC converter generates the rectified form of the desired phase voltage and the H-bridge inverter alternates and controls the polarity of the output voltage. With the help of this topology phase voltages are independently adjusted, resulting in a faster excitation and demagnetization; hence, a high-performance current regulation is achieved even with a longer dwell angle and two-phase excitation for a wide range of operating conditions. Therefore, the commutation performance is improved, a more balanced excitation than the traditional method is achieved. As a result, torque ripple is reduced and the average torque production is improved. Moreover, since the voltage is always regulated dynamically, large DC bus capacitors are no longer needed and the cost and the size of the drive system are reduced, as well as the capacitor induced losses are reduced. The comparative simulation studies performed in MATLAB®/Simulink® validated the superiority of the proposed system. The proposed SRM drive system reduced the torque ripple from 46.8 % to 6.3 %, increased the average torque from 20 Nm to 21.5 Nm at the rated speed and peak phase current condition. Extended simulation results for a wider speed range validated the proposed system's superiority in terms of torque ripple reduction, torque per ampere ratio, and output power improvements. A future study may focus on a torque distribution study to enhance the proposed drive system's performance at even higher levels.

## Acknowledgment

This research is supported by The Scientific and Technological Research Council of Turkey (TUBITAK) under Grant 118E172.

## Conflict of Interest

The author has no conflicts of interest to declare.

**Similarity (iThenticate):** %12

## References

[1] R. Krishnan, Switched Reluctance Motor Drives: Modeling, Simulation, Analysis, Design, and Applications. CRC Press/Taylor & Francis Group, Boca Raton, FL, 2001.

[2] B. Bilgin, J. W. Jiang, and A. Emadi, Switched Reluctance Motor Drives. CRC Press/Taylor & Francis Group, Boca Raton, FL, 2019.

[3] Y. Yasa, D. Tekgun, Y. Sozer, J. Kutz, and J. Tylenda, Effect of distributed airgap in the stator for acoustic noise reduction in switched reluctance motors, IEEE Applied Power Electronics Conference and Exposition (APEC), page 633-639, Tampa, FL, USA, 26-30 March 2017.

[4] T. Husain, Y. Sozer, and I. Husain, DC-Assisted bipolar switched reluctance machine, IEEE Trans. Ind. Appl., 53 (3), 2098–2109, 2017, https://doi.org/10.1109/tia.2017.2675363.

[5] Y. Sozer and D. A. Torrey, Optimal turn-off angle control in the face of automatic turn-on angle control for switched-reluctance motors, IET Electr. Power Appl., 1 (3), 395, 2007, https://doi.org/10.1049/iet-epa:20060412.

[6] H.-N. Huang, K.-W. Hu, and C.-M. Liaw, Switch-mode rectifier fed switched-reluctance motor drive with dynamic commutation shifting using DC-link current, IET Electr. Power Appl., 11 (4), 640–652, 2017, https://doi.org/10.1049/iet-epa.2016.0783.

[7] T. Husain, A. Elrayyah, Y. Sozer, and I. Husain, Unified control for switched reluctance motors for wide speed operation. IEEE Trans. Ind. Electron., 66 (5), 3401–3411, 2019, https://doi.org/10.1109/tie.2018.2849993.

[8] T. Husain, A. Elrayyah, Y. Sozer, and I. Husain, Flux-weakening control of switched reluctance machines in rotating reference frame. IEEE Trans. Ind. Appl., 52 (1), 267–277, 2016, https://doi.org/10.1109/tia.2015.2469778.

[9] H. C. Chang and C. M. Liaw, Development of a compact switched-reluctance motor drive for EV propulsion with voltage-boosting and PFC charging capabilities. IEEE Trans. Veh. Technol., 58 (7), 3198–3215, 2009, https://doi.org/10.1109/TVT.2009.2017546.

[10] C. Gan, J. Wu, Y. Hu, S. Yang, W. Cao, and J. M. Guerrero, New integrated multilevel converter for switched reluctance motor drives in plug-in hybrid electric vehicles with flexible energy conversion. IEEE Trans. Power Electron., 32 (5), 3754–3766, 2017, https://doi.org/10.1109/TPEL.2016.2583467.

[11] K. W. Hu, P. H. Yi, and C. M. Liaw, An EV SRM Drive powered by battery/supercapacitor with G2V and V2H/V2G capabilities. IEEE Trans. Ind. Electron., 62 (8), 4714–4727, 2015, https://doi.org/10.1109/tie.2015.2396873.

[12] J. W. Ahn, S. J. Park, and D. H. Lee, Hybrid excitation of SRM for reduction of vibration and acoustic noise. IEEE Trans. Ind. Electron., 51 (2), 374–380, 2004, https://doi.org/10.1109/tie.2004.825227.

[13] A. K. Jain and N. Mohan, SRM power converter for operation with high demagnetization voltage. IEEE Trans. Ind. Appl., 41 (5), 1224–1231, 2005, https://doi.org/10.1109/TIA.2005.853390.

[14] K. Tomczewski and K. Wrobel, Improved C-dump converter for switched reluctance motor drives, IET Power Electron., 7 (10), 2628–2635, 2014, https://doi.org/10.1049/iet-pel.2013.0738.

[15] K.-W. Hu, J.-C. Wang, T.-S. Lin, and C.-M. Liaw, A switched-reluctance generator with interleaved

interface DC–DC converter. IEEE Trans. Energy Convers., 30 (1), 273–284, 2015, https://doi.org/10.1109/tec.2014.2333585.

[16] Y. H. Yoon, S. H. Song, T. W. Lee, C. Y. Won, and Y. R. Kim, High performance switched reluctance motor drive for automobiles using C-dump converters. IEEE Int. Symp. Ind. Electron., 2, 969–974, 2004, https://doi.org/10.1109/isie.2004.1571945.

[17] A. K. Jain and N. Mohan, SRM power converter for operation with high demagnetization voltage, IEEE Trans. Ind. Appl., 41 (5), 1224–1231, 2005, https://doi.org/10.1109/tia.2005.853390.

[18] R. Krishnan, S. Y. Park, and K. Ha, Theory and operation of a four-quadrant switched reluctance motor drive with a single controllable switch - The lowest cost four-quadrant brushless motor drive. IEEE Trans. Ind. Appl., 41 (4), 1047–1055, 2005, https://doi.org/10.1109/tia.2005.851019.

[19] H. Chang and C. Liaw, An integrated driving/charging switched reluctance motor drive using three-phase power module. IEEE Trans. Ind. Electron., 58 (5), 1763–1775, 2011, https://doi.org/10.1109/tie.2010.2051938.

[20] Q. Sun, J. Wu, C. Gan, J. Si, J. Guo, and Y. Hu, Cascaded multiport converter for SRM-based hybrid electrical vehicle applications, IEEE Trans. Power Electron., 34 (12), 11940–11951, 2019, https://doi.org/10.1109/tpel.2019.2909187.

[21] T. Kim, W. Qiao, and L. Qu, Power electronics-enabled self-X multicell batteries: A design toward smart batteries, IEEE Trans. Power Electron., 27 (11), 4723–4733, 2012, https://doi.org/10.1109/tpel.2012.2183618.

[22] L. Liu, H. Li, S.-H. Hwang, and J.-M. Kim, An energy-efficient motor drive with autonomous power regenerative control system based on cascaded multilevel inverters and segmented energy storage, IEEE Trans. Ind. Appl., 49 (1), 178–188, 2013, https://doi.org/10.1109/tia.2012.2229687.

[23] H. Li, B. Bilgin, and A. Emadi, An improved torque sharing function for torque ripple reduction in switched reluctance machines. IEEE Trans. Power Electron., 34 (2), 1635–1644, 2019, https://doi.org/10.1109/tpel.2018.2835773.

[24] J. Ye, B. Bilgin, and A. Emadi, An offline torque sharing function for torque ripple reduction in switched reluctance motor drives. IEEE Trans. Energy Convers., 30 (2), 726–735, 2015, https://doi.org/10.1109/tec.2014.2383991.

[25] T. Husain, A. Elrayyah, Y. Sozer, and I. Husain, Flux-weakening control of switched reluctance machines in rotating reference frame. IEEE Trans. Ind. Appl., 52 (1), 267–277, 2016, https://doi.org/10.1109/tia.2015.2469778.

[26] J. Sun, G.-Z. Cao, S.-D. Huang, Y. Peng, J. He, and Q.-Q. Qian, Sliding-mode-observer-based position estimation for sensorless control of the planar switched reluctance motor. IEEE Access, 7, 61034–61045, 2019, https://doi.org/10.1109/access.2019. 2913702.

[27] H. N. Huang, K. W. Hu, Y. W. Wu, T. L. Jong, and C. M. Liaw, A current control scheme with back emf cancellation and tracking error adapted commutation shift for switched-reluctance motor drive. IEEE Trans. Ind. Electron., 63 (12), 7381–7392, 2016 , https://doi.org/10.1109/tie.2016.2594168.

[28] M. Pittermann, J. Fort, J. Diesl, and V. Pavlicek, Converters for switched reluctance motor - topology comparison, Proc. 2018 18th Int. Conf. Mechatronics - Mechatronika, Brno, Czech Republic, 5-7 Dec. 2018.